

# Numerical Analysis of Stent Porosity and Strut Geometry for Intra-saccular Aneurysmal Flow

Jingliang Dong<sup>1</sup>, Kelvin KL Wong<sup>1</sup>, Zhonghua Sun<sup>2</sup>, Jiyuan Tu<sup>1</sup>

<sup>1</sup>School of Aerospace, Mechanical & Manufacturing Engineering, and Health Innovations Research Institute, RMIT University, Australia

<sup>2</sup>Discipline of Medical Imaging, Department of Imaging and Applied Physics, Curtin University of Technology, Australia

## Abstract

*We numerically simulate the hemodynamics of aneurysmal flow and evaluate stent design configuration based on an idealistic geometrical model. We examined large-scale swirling of blood within a significantly dilated aneurysm. Various parameters such as stent porosity and strut shape have an impact on the pressure and shear strain rate within the aneurysm. Using biofluid mechanical parameters such as pressure gradient and shear strain rate for aneurysmal arteries implanting with different stent configuration, a flow analysis framework for evaluation of stents is developed. With the application of cardiac flow analysis, we aim to achieve a balance in the two properties in order to prevent aneurysmal rupture and thrombosis formation and give out the most suitable stent configuration for the stent implanting surgery.*

## 1. Introduction

Aneurysm is a blood filled dilation that is caused by atherosclerotic disease of blood vessel walls and is common near the branches of intracranial arteries. With aging, aneurysms increase in size resulting in the rupture and initiation of bleeding within the brain. This causes a medical condition known as stroke that can result in death or disability. Hemorrhagic stroke is known to be one of the common causes of death by cardiovascular disease and affects 15% of stroke patients in the world's population [1]. The causes of this cardiovascular disease are diabetes, obesity, alcoholism, tobacco use and copper deficiency [2]. Patients who die from such a medical condition have copper deficiency of approximately quarter quantity of a normal person. It might be worthwhile noting that tobacco and alcohol intake diminishes the copper content within the body, resulting in the progression of aneurysmal growth as portrayed by [3]. Hemorrhagic stroke develops when bleeding is present within the brain. The ischaemic and hemorrhagic stroke conditions account for 85% and 15% of cases respectively. One cause of bleeding is the

rupture of aneurysm in the atherosclerotic blood vessel. Therefore, it is of interest to investigate stent deployment and optimization of stent design to research in the initiation and progression of an aneurysm leading to its final rupture. The affected arterial region is generally treated using angioplasty with stents or by open surgery that consist of clipping whereby a clip is inserted across the aneurysm in order to prevent blood from entering the aneurysmal bulge and aggravating its dilation.

In particular, based on numerical simulation, we can study the change in intra-aneurysmal flow field for a diseased artery implanting with different stent porosities and strut shapes. Pressure gradient and shear strain mapping can be performed by processing the simulation results and used to analyze the flow in the aneurysm sac. To quantify the complex aneurysmal flow, a monitor point collects the fluid mechanical values at the center of the sac. Information from these flow characteristics relate to the stress and strain due to swirling of the blood within an aneurysm. This paper presents the use of computational fluid dynamics to simulate the evolution of this aneurysmal flow for both the non-stented and stented arterial with various types of configuration. This information can assist us in optimizing the stent configuration such that aneurysm growth can be minimised as much as possible.

### 1.1. Computational fluid dynamics

The governing equations for viscous, incompressible fluid flow can be written using Navier–Stokes equations and mass continuity equation as

$$\rho L \frac{dV}{dt} = \rho L g + \mu \nabla^2 V - \nabla P, \quad (1)$$

$$\frac{\delta \rho L}{\delta t} + (\nabla \cdot V) \rho L = 0, \quad (2)$$

where  $V$  is the fluid velocity vector.  $\mu$  is the viscosity,  $g$  is the gravitational acceleration,  $\rho$  is the density, and  $P$  is the dynamic pressure of the fluid. Vortices that exist in a

stented aneurysm may be driven by orifice or aneurysm flow [4]. Numerical simulation of flow in stented aneurysms is performed in various studies. In particular, the use of Lattice Boltzmann approach is heavily implemented [4-6]. Numerical simulation based on untreated and stented aneurysmal arteries with various strut shapes and stent porosities may be performed to investigate their difference in terms of blood flow. The modelling of circular, ellipse, triangular, and rectangular stent struts with different porosities were considered in this work. Stent porosities configuration based on 3, 4, 5, 6 and 7 struts at the neck of the aneurysm are implemented.

## 1.2. Post-processing of simulated flow

For aneurysmal flow, there exists a force which propels blood into the aneurysmal sac. This force is proportional to the difference in blood pressure from the vessel to the aneurysm across its neck. The pressure gradient  $\nabla P$  is therefore influenced by the resistance to that flow. The factors determining this resistance are functionally the dimension of the aneurysmal neck, and in the case of stenting, it will be the effective orifice area of the neck and excludes the stent strut areas.

In a fluid flow that is incompressible and under a steady flow field, the shear strain rate of a material fluid element is defined as the rate of decrease of the angle formed by two mutually perpendicular lines on the element. As such, the shear strain rate  $\dot{\gamma}$  is defined as a function of shear stress  $\tau$  and is proportional to the velocity gradient in the perpendicular direction of the flow:

$$\dot{\gamma} = f(\tau) = -\frac{du}{dy}. \quad (3)$$

In general, the shear strain rate can be defined as a function of  $\tau$ , and we establish a linear relationship between the shear stress and strain components with the viscosity as its gradient. Mathematically, the model can be expressed as

$$\tau = \mu \dot{\gamma}, \quad (4)$$

where  $\mu$  is the viscosity of the fluid.

## 2. Experimental setup

The computational domain of the aneurysmal model is shown in Figure 1. The diameters for parent vessel and the aneurysmal sac are both 4 mm. The flow will enter the vessel with no obstacle and swirl within the aneurysm. For the stented artery, the aneurysmal flow velocity is reduced due to the stent struts obstructing blood movement. In this work, we introduced a pulsatile inlet velocity boundary condition, which is normal to the inlet surface for investigating the effects of momentum variations with various stent struts configuration [5] (Figure 2.). The artery is modelled to be long enough so that towards the exit of the vessel, the zero pressure gradient boundary condition along the length of the artery is implemented.

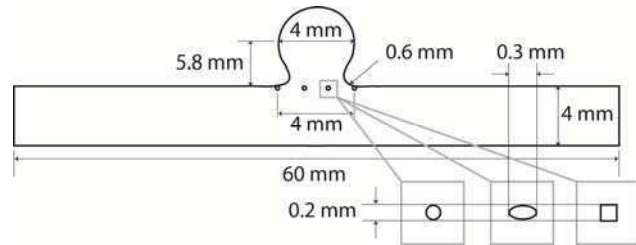


Figure 1. Dimensions of aneurysm and stent struts.

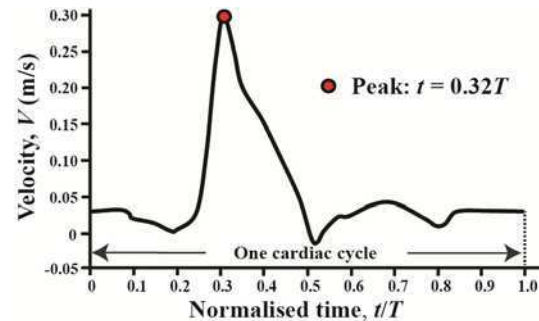


Figure 2. Inlet velocity waveform.

A mesh size of more than 12,000 cells is generated for the flow domain. A mesh independence study has also been carried out to ascertain that the selected domain size is sufficient in resolving the flow gradients.

After the processing of geometrical mesh, the next step in the preprocessing stage of the CFD workflow is to define and subsequently, implement the inputs for the physical models and boundary conditions. Here, we have assumed that flow of blood through the arterial vessel is incompressible, homogeneous, laminar, and Newtonian. The fluid properties are reported in Table 1. It may be worthwhile noting that Reynolds number in the cerebral artery typically has a range of 100 to 300, and is less than 30 within the aneurysm [6]. To model the unsteady nature of the flow field, transient CFD simulation was performed. For simplicity, the artery wall is treated as rigid and non slipping.

Table 1. Fluid properties used in numerical simulation.

Parameters	Values	Units
Dynamic viscosity	$3.5 \times 10^{-3}$	Pa·s
Density	1060	$\text{kg}\cdot\text{m}^{-3}$

Software ANSYS CFX 12 has been utilized for transient computational fluid dynamic simulations. The discretization of Navier Stokes equation is based on coupling both finite element and finite-volume approaches. The flow in the vessel is simulated for 5 cardiac cycles. A fully implicit scheme with a fixed time computational time step (0.01 s) was set for the transient simulations. For each time step, satisfactory convergence

criteria with  $1 \times 10^{-4}$  root mean square residual for all variables should be achieved.

### 3. Results

We have investigated the intra-aneurysmal flow field in terms of streamline tracing, pressure gradient and shear strain rate at the peak of the inlet velocity profile ( $t=3.32s$ ), comparing the non-stented artery, all of the results give a good demonstration for reveal the effects of different stenting strategies on the flow status inside the secular aneurysm.

Streamline tracing is used to deduce the path of the blood flow. To get a more clearly intra-aneurysmal vortex structure, we place the streamline right begin from a specific point, which coordinates are  $(4 \times 10^{-9}, 5.5 \times 10^{-3}, 1 \times 10^{-3})$ , after then obviously defined large-scale vortex for the stented arteries are presented in the aneurysm sac as shown in Figure 3. The results show that the entire counter-clockwise intra-aneurysmal vortex reduces in strength for all the stenting configurations. For the particular stent strut shape, the vortex strength is reduced as the increasing of the stent porosity. For the same stent porosity configuration, the rectangular and triangular stent strut same to be the much more effective vortex decreasing strut shape than the others.

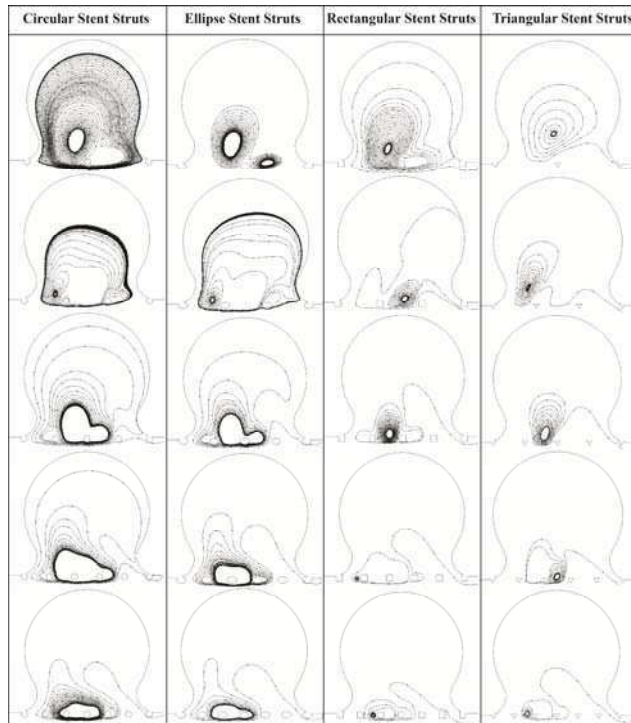


Figure 3. Streamline tracing for stented arteries shows that the primary vortex varies in size based on the circular, ellipse, rectangular and triangular stent struts.

In our previous work, we have compared the contours of pressure gradient and shear strain rate for investigating

the stenting effect on the intra-aneurysmal flow, however, the contours of pressure gradient and shear strain rate are still not clearly enough for us to compare the differences among these treating plans. In order to get the variation trends between these flow parameters and stent strut shape and stent porosity, we using the same monitor point ( $4 \times 10^{-9}, 5.5 \times 10^{-3}, 1 \times 10^{-3}$ ) to extract data for comparison analysis.

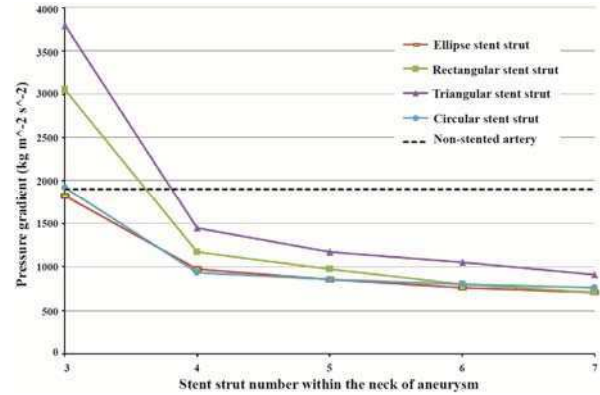


Figure 4. Chart of pressure gradient variation at the monitor point inside the aneurysm sac for different stenting strategies.

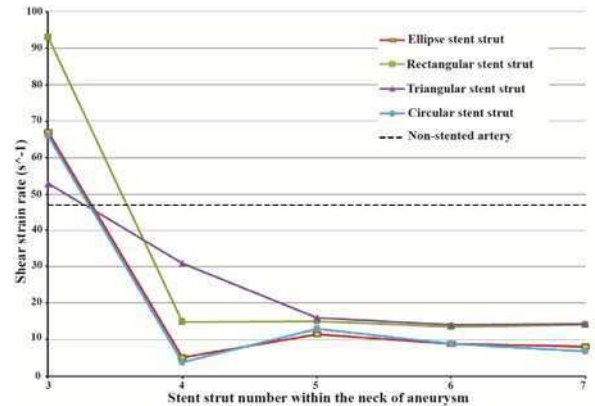


Figure 5. Chart of shear strain rate variation at the monitor point inside the aneurysm sac for different stenting strategies.

According with the pressure gradient value of the monitor point inside the secular aneurysm for the non-stented artery ( $\nabla P=1900 \text{ kg}\cdot\text{m}^{-2}\cdot\text{s}^{-2}$ ), after stenting with 3 struts between the neck of the aneurysm, the pressure gradient changing for these four types of stent shows out two different kinds of variation tendency. Both of the triangular shape ( $\nabla P=3800 \text{ kg}\cdot\text{m}^{-2}\cdot\text{s}^{-2}$ ) and rectangular shape ( $\nabla P=3050 \text{ kg}\cdot\text{m}^{-2}\cdot\text{s}^{-2}$ ) strut cause significant value jump, which are 100% value jump for triangular strut, 60% value increase for rectangular strut. While the rest types of strut, circular and ellipse struts, only contribute small pressure gradient variations at 1% ( $\nabla P=1920 \text{ kg}\cdot\text{m}^{-2}\cdot\text{s}^{-2}$ ) and 4% ( $\nabla P=1820 \text{ kg}\cdot\text{m}^{-2}\cdot\text{s}^{-2}$ ) respectively. With

increasing the struts number, all of the strut shapes behave a decline tendency and drop the  $\nabla P$  value below the non-stented artery. The pressure gradient value of the monitor point for triangular stenting maintain to be larger than the other three types of stenting from 3 struts to 6 struts, and when 7 stent struts has been placed at the aneurysmal neck, every stenting configuration illustrate a deeply low pressure gradient value and lead to a 52%  $\nabla P$  drop at least.

The same decline nature exists for the shear strain rate variation. When the artery is not stented, the shear strain rate value is holding at  $47 \text{ s}^{-1}$ . After being inserted 3struts stent, all kinds of the stent cause value increases, where rectangular stenting causes a 97.9% increase ( $\dot{\gamma}=93 \text{ s}^{-1}$ ), triangular stenting leads to a 12.7% increase ( $\dot{\gamma}=53 \text{ s}^{-1}$ ), circular and ellipse stenting contribute 40% ( $\dot{\gamma}=66 \text{ s}^{-1}$ ) on the value grow. As implanting more stent struts from 4 to 7, the decline trends for those four types of stent become more smooth and slow. In particular, the rectangular stenting and triangular stenting maintain a higher shear strain rate level than the circular and ellipse stenting configuration, and the representations of circular and ellipse stenting keep almost the same variation tendency.

#### 4. Discussion

Based on numerical simulation and flow analysis, we are able to characterize flow fields on untreated and stented aneurysmal arteries. The streamline tracings enable the visualization of strength and position of a large-scale vortex in an aneurysmal sac. The results demonstrate that the stenting causes a reduction of pressure, velocity, vorticity shear rate. Reduced pressure exerted by blood on the aneurysmal sac will decrease the risk of rupture. However, lower volume of flow into the sac increases the viscosity of blood in the aneurysm [6]. Reduced vorticity in the sac also corresponds to a lower fluid shear stress and shear strain rate. Note that high shear stress is necessary for preventing platelet-dependent thrombosis [7]. Moreover, reduced blood into the aneurysm also means flow stagnancy and the induction of thrombosis increases. All these undesirable conditions will aggravate aneurysm rupture [8]. Therefore, the triangular stenting with 4 struts configuration deployed may be of sufficient porosity to minimise aneurysmal rupture [6] but prevent platelet aggregation among all the investigated treating strategies. The study of fluid mechanical properties in non-stented and stented aneurysmal flow can enable medical experts to evaluate the effectiveness of stent designs and their corresponding porosities in prevention of aneurysm dilation leading to rupture.

#### 5. Conclusion

In this paper, we present a simulated model to show stenting inside the diseased artery at the entrance of the aneurysm, and demonstrate that the circular and ellipse stent struts configuration can minimise aneurysmal rupture

risk. On the contrary, the rectangular and triangular stent struts are the best for preventing platelet aggregation. Therefore, there is no ideal stent design. We can only optimize the aneurysmal rupture and prevent thrombosis based on appropriate strut shape geometry.

#### Acknowledgements

The financial support provided by the Australian Research Council (ARC project ID DP0986183) is gratefully acknowledged.

#### References

- [1] Australia's Health 2008. Number AUS 99. Australian Institute of Health and Welfare, 2008.
- [2] Valencia A, Morales H, Rivera R, Bravo E, Galvez M. Blood flow dynamics in patient-specific cerebral aneurysm models: The relationship between wall shear stress and aneurysm area index. *Medical Engineering & Physics* 2008;30:329–340.
- [3] Utter B, Rossmann JS. Numerical simulation of saccular aneurysm hemodynamics: Influence of morphology on rupture risk. *Journal of Biomechanics* 2007;40:2716–2722.
- [4] Hirabayashi M, Ohta M, Barath K, Rufenacht DA, Chopard B. Numerical analysis of the flow pattern in stented aneurysms and its relation to velocity reduction and stent efficiency. *Mathematics and Computers in Simulation* 2006;72:128–133.
- [5] Xu X, Lee JS. Application of the lattice boltzmann method to flow in aneurysm with ring-shaped stent obstacles. *Int J Num Meth Fluids* 2008;59:691–710.
- [6] Kim YH, Xu X, Lee JS. The effect of stent porosity and strut shape on saccular aneurysm and its numerical analysis with lattice boltzmann method. *Ann Biomed. Eng* 2010; 38:2274–2292.
- [7] Sukavaneshvar S, Rosa GM, Solen KA. Enhancement of stent-induced thromboembolism by residual stenoses: contribution of hemodynamics. *Ann Biomed Eng* 2000; 28:182–193.
- [8] Liou TM, Liou SN. Pulsatile flows in a lateral aneurysm anchored on a stented and curved parent vessel. *Experimental Mechanics* 2004;44:253–260.

Address for correspondence.

Prof Jiyuan Tu

School of Aerospace, Mechanical and Manufacturing Engineering, and Health Innovations Research Institute (HIRI), RMIT University, VIC 3083, Australia

Email: Jiyuan.Tu@rmit.edu.au.